RSC Advances

This article can be cited before page numbers have been issued, to do this please use: W. Kim, M. Cheon, S. Lee, T. Lee, J. J. Park, C. R. Cho, C. H. Park, I. Takeuchi and S. Jeong, *RSC Adv.*, 2016, DOI: 10.1039/C6RA05746B.

ROYAL SOCIETY OF CHEMISTRY

www.rsc.org/advances

View Article Online
DOI: 10.1039/C6RA05746B

RSC Advances

PAPER

Magnetic domains in H-mediated $Zn_{0.9}Co_{0.1}O$ microdisk arrays

Won-Kyung Kim, [a,†,‡] Miyeon Cheon, [b,†] Seunghun Lee, [c] Tae-Woo Lee, [d] Jung Jin Park, [e] Chae Ryong Cho, [f] Chul Hong Park, [g] Ichiro Takeuchi, [c] and Se-Young Jeong [a,h] *

Received 00th January 20xx,
Accepted 00th January 20xx

DOI: 10.1039/x0xx00000x

www.rsc.org/

In this study, we have fabricated and studied magnetic domains in the periodic H-mediated $Zn_{0.9}Co_{0.1}O$ (H-ZCO) microdisk structures at room temperture with MFM technique. The results of MFM show that the z-componet of the remanent magnetic moment is uniform even though the value is much smaller than that of the saturation magnetic monent. In the investigation of H-ZCO microdisk arrays in different volumes, the magnetic domains observed on different sizes of the H-ZCO microdisks exhibited same magnetic domain characteristics perpendicular magnetization, regardless of the volume. Also, we confirmed that the ferromagntism in H-ZnCoO system is mediated by hyrogens with MFM results of ZnCoO hydrogen injected and dehydrogenated.

Introduction

The development of high-speed, nonvolatile spin devices with low power consumption is essential for the realization of next-generation information and communication technologies.[1,2] Studies of spintronics based on magneto-electrics, with various micro- and nano-sized architectures in metals or semiconductors, have facilitated information access, transfer, and novel storage techniques.[3-5] Extensive research on meso-structured magnetic domains has been performed primarily on ferromagnetic metals, such as permalloy (Ni–Fe),[6-10] supermalloy (Ni-Mo-Fe), [11] Co,[12] Co-Pt,[13,14] and Co-Ni.[15] In addition to these magnetic domain control techniques in metals, recent efforts have been made to merge them with highly developed modern microelectronics and optoelectronics, based on semiconductors. Such an interdisciplinary application is expected to be realized using precisely structured magnetic domain configurations in magnetic impurity-doped semiconductors.[16-18]

Intrinsic ferromagnetic characteristics, magnetization switching, and spin transport techniques for spintronic applications have been reported in a magnetic semiconductor, GaMnAs.[17-19] However, due to its low Curie temperature, GaMnAs-based spintronic devices only operate below ~100 K.[16-19] Researchers have investigated numerous materials in an effort to find novel spin-device materials that work at room temperature; transition metal-doped oxides, such as ZnO and TiO_2, have attracted considerable interest.[20-31] Among these materials, transition-metal-doped ZnO (TM:ZnO) has been regarded as a promising candidate for spintronic devices, even the reproducibility, reliability and origin of its room temperature ferromagnetism are still debated offering room-temperature ferromagnetism.[25-31]

Some groups observed magnetic domains in TM:ZnO thin films or nanofibers and the observed magnetic domain sizes were less than 1 μm either the samples were micron-size patterned or not.[32-34] Recently, we observed localized ferromagnetic domains in paramagnetic ZnCoO where the ferromagnetic domains were formed by selective hydrogen exposure with anodic aluminum oxide template. The magnetic domains were randomly distributed in plane and the size was about 250 nm.[35]

In this report, we have fabricated and studied magnetic domains in the periodic ZnCoO microdisk structures at room temperture with MFM technique. The results of MFM shows that the z-componet of the remanent magnetic moment is uniform even though the value is much smaller than the saturation magnetic monent. In order to confirm the geometrical dependence of magnetic domains, we fabricated different volumes of H-ZCO microdisks, and investigated the magnetic domains as a function of geometry.

[a] Department of Cogno-mechatronics Engineering, Pusan National University, Miryang, 627-706, Republic of Korea.
[b] Crystal Bank Research Institute, Pusan National University, Miryang, 627-706, Republic of Korea.
[c] Department of Materials Science and Engineering, University of Maryland, College Park, MD 20742, USA.
[d] KAIST Analysis Center for Research Advancement, Daejeon, 305-701, Republic of Korea.
[e] Department of Aerospace Engineering, University of Maryland, College Park, MD 20742, USA.
[f] Department of Nano Fusion Technology, Pusan National University, Miryang, 627-706, Republic of Korea.
[g] Department of Physics Education, Pusan National University, Busan, 609-735, Republic of Korea.
[h] Department of Optics and Mechatronics Engineering, Pusan National University, Miryang, 627-706, Republic of Korea.
† Both authors contributed equally to this work.
‡ Current address: R&D Center, LG Display Co., Ltd., Paju, 413-779, Republic of Korea
* Corresponding author: E-mail: syjeong@pusan.ac.kr; Fax: +82-55-353-1314; Tel: +82-55-350-5273.

View Article Online
DOI: 10.1039/C6RA05746B

Experimental

Co-doped ZnO microdisks were prepared using UV lithography and the lift-off process. Photoresist (AZ1512, AZ Electronic Materials) was coated onto an Al_2O_3 (0001) substrate, and inverse micro-sized patterns were transferred using UV lithography. A ZnCoO layer was deposited at 100 °C using radio-frequency sputtering of a 10 mol% Co-doped ZnO polycrystalline target, followed by subsequent removal of the sacrificial photoresist layer. Undesirable protrusions along the circumference of the microdisk and photoresist residues were removed via reactive ion etching with Ar and O_2 gases. To introduce and remove magnetic characteristics, hydrogen was injected into the manufactured ZnCoO microdisk using HIP with Ar:H_2 mixed gas (9:1 vol%) at 300 °C for 10 h and hydrogen was removed (ejected) from the ZnCoO microdisk by annealing at 500 °C in a vacuum atmosphere for 2 h. The crystalline structure of ZnCoO and its surface morphology were analyzed using X-ray diffraction (XRD, Empyrean, PANalytical), scanning electron microscopy (SEM, S4700, Hitachi), transmission electron microscopy (TEM, Tecnai TF300 ST, FEI company), and atomic force microscopy (AFM, XE-100, Park Systems). Reversible manipulation between paramagnetism and ferromagnetism, saturation magnetization, and magnetic anisotropy were investigated using vibrating sample magnetometry (VSM, Physical Property Measurement System, Quantum Design). The magnetic domain structure was observed using magnetic force microscopy (MFM, XE-100, Park Systems), equipped with a PPP-MFMR cantilever tip (Nanosensors) and lift mode; the tip-to-sample distance was 30 nm for effective magnetic-phase scanning. The magnetic domain simulation was carried out using an object-oriented micromagnetic framework (National Institute of Standards and Technology).

Results and discussion

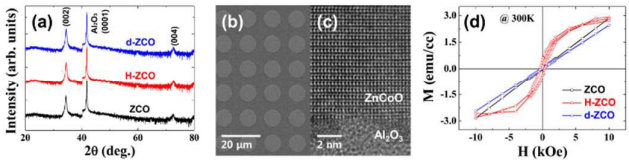

Fig. 1 (a) X-ray diffraction (XRD) patterns of as-grown ZnCoO (ZCO), hydrogen-injected ZCO (H-ZCO), and dehydrogenated H-ZCO (d-ZCO). No peaks corresponding to cobalt precipitation were observed. (b) Scanning electron microscopy (SEM) image of a H-ZCO microdisk array. (c) Cross-sectional high-resolution transmission electron microscopy (HRTEM) image of a single H-ZCO microdisk. (d) Magnetization–magnetic field (*M–H*) curves of the ZCO series, showing reversible manipulation of room-temperature ferromagnetism by hydrogen injection and ejection processes.

Figure 1 shows the change in the structural and magnetic characteristics of the ZnCoO before and after hydrogen injection/ejection processes. As-grown ZnCoO, hydrogen-injected ZnCoO, and dehydrogenated ZnCoO are abbreviated as ZCO, H-ZCO, and d-ZCO, respectively. X-ray diffraction (XRD) patterns shown in Fig. 1(a) reveal that the crystal orientations of ZCO, H-ZCO, and d-ZCO are in c-axis and not significantly affected by the hydrogenation and the dehydrogenation. XRD patterns were measured for other pieces which were a part of the same sample as the microdisk array pieces. Figure 1(b) shows a scanning electron microscopy (SEM) image of an H-ZCO array. The diameter and pitch of the well-defined microdisk array are both 7 μm. The cross-sectional high-resolution transmission electron microscopy (HRTEM) image in Fig. 1(c) shows the lattice image pattern of a H-ZCO microdisk. From XRD results and the HRTEM image taken of several regions in the H-ZCO microdisk array, we confirmed that Co^{2+} ions were substituted for Zn^{2+} ions; no secondary phases related to Co-metal clusters or cobalt oxide species were observed after the hydrogenation process.[30,31,36] The field-dependent magnetization along the out-of-plane axis exhibited a distinct transition from the paramagnetic to the ferromagnetic state and vice versa, with hydrogen injection/ejection, as shown in Fig. 1(d). The diamagnetic contribution of the Al_2O_3 substrate was subtracted by independent measurement; unintended ferromagnetic signals from external factors were prevented with careful handlings. Before hydrogen injection, ZCO exhibited ordinary paramagnetic behavior; however, following hydrogen injection, strong ferromagnetic spin–spin ordering of Co^{2+} ions on H-ZCO was induced, as identified by the resulting room-temperature hysteresis.[25-31] To remove ferromagnetic spin-ordering on H-ZCO, hydrogen was ejected via a high-vacuum annealing process, which prevented chemical oxidation. After hydrogen ejection, the ferromagnetism of d-ZCO disappeared. This reversible manipulation of magnetic characteristics indicates that the room-temperature ferromagnetism of H-ZCO is induced by hydrogen mediation, not by defects or Co-metal clusters.

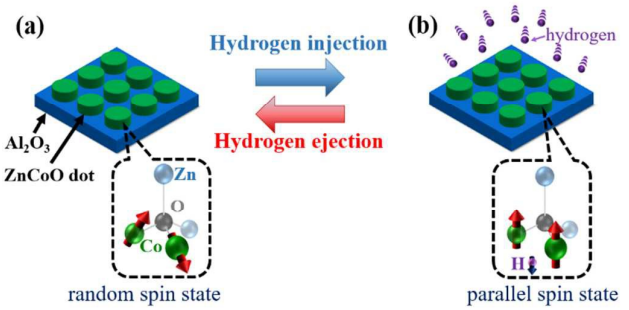

Fig. 2 Schematic diagram for the ferromagnetism in a ZCO microdisk array. The Wurzite crystal structure of ZnO doped with Co is shown inside of the dashed line- rectangular. Zn ions are in light blue, oxygen in gray, Co in green, and H in purple. The red and blue arrows represent spin of Co ions and of hydrogen ion, respectively. (a) Before hydrogen injection or after hydrogen ejection, spins of neighboring Co^{2+} impurities point in random directions. (b) After hydrogen injection, hydrogen mediates a short-range ferromagnetic interaction between neighboring Co^{2+} impurities, which results ferromagnetism in H-ZCO.

The mechanism for the ferroamgnetism in H-ZnCoO was well explained in the reference 25. Interstitial hydrogens mediate a strong short-ranged ferromagnetic spin-spin interaction between neighboring Co^{2+} impurities through the formation of a bridge bond as shown in Fig 2. After hydrogen injection, hydrogen mediates a ferromagnetic interaction between neighboring Co^{2+} impurities,

View Article Online
DOI: 10.1039/C6RA05746B

which results ferromagnetism in H-ZCO, while the spin of Co^{2+} ions points randomly without hydrogen.

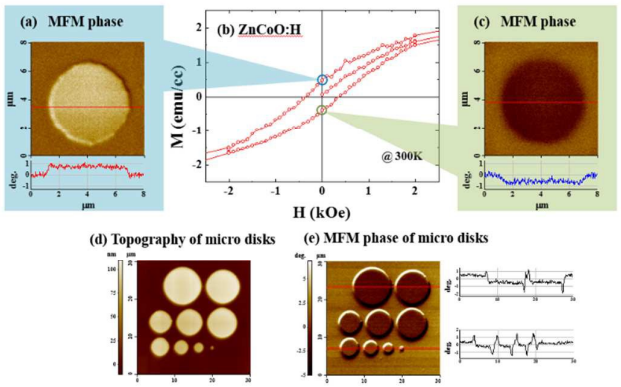

Fig. 3 MFM results (a) and (c) of a H-ZCO microdisk corresponding to certain positions along the *M–H* curve (b). MFM image (a) in the absence of an external magnetic field after applying an external magnetic field of +1000 Oe and (c) in the absence of an external magnetic field after applying an external magnetic field of −1000 Oe to reverse the spin-ordering along the out-of-plane direction. (d), (e) AFM and MFM results of microdisks with different sizes, respectively.

Since the remanent magnetization is much smaller than the saturation magnetization, we expected mutidomain MFM images. The observed MFM results were shown in Fig 3. As shown in Fig 3 (a) and (c), the magnetic domains were unifrom. Also, the reversal of MFM phases in a H-ZCO microdisk was observed using an external magnetic field larger than its coercive field (Fig. 3). After applying a 0.1-T external magnetic field to H-ZCO along the out-of-plane direction using a magnetic field generator, MFM phase images were scanned in the absence of the external magnetic field at room temperature. The reversed external magnetic field was then applied and removed. The resulting perpendicular magnetization of the H-ZCO micro-dot had the opposite phase direction; its up magnetic phase in Fig. 3(a) differs from down state in Fig. 3(c) by ~2° from its line profiles.

The effect of structural factors on micro-sized magnetic domain was not elaborately analyzed, but it is interesting result that H-ZCO microdisk could maintain the uniform out-of-plane magnetic moment in the absence of the external magnetic field. This notable perpendicular magnetization in H-ZCO microdisk could be applied to perpendicular magnetic recording for enhancing information storage density.

As in the previous report, hundreds nanometer sized magnetic domains on ZnCoO:H thin film showed the in-plane magnetic moment after removing the in-plane external magnetic field of 1000 Oe.[35] In contrast to selectively hydrogen injected thin film system, a magnetic domain of localized structure system showed the uniform out-of-plane component without the external magnetic field, which might be affected by geometry and strain of structures rather than the energetic stability of Co-H-Co complexes in ZnCoO:H. In order to confirm the geometrical dependence of magnetization, we tried to fabricate different volumes of H-ZCO microdisks, and investigated the magnetic domain characteristics as a function of geometry. We fabricated H-ZCO microdisks having different volumes. The diameters of microdisk were controlled from 2 μm to 10 μm. In MFM phase images as shown in Fig 2(d), all of the H-ZCO microdisk exhibited perpendicular magnetization, which

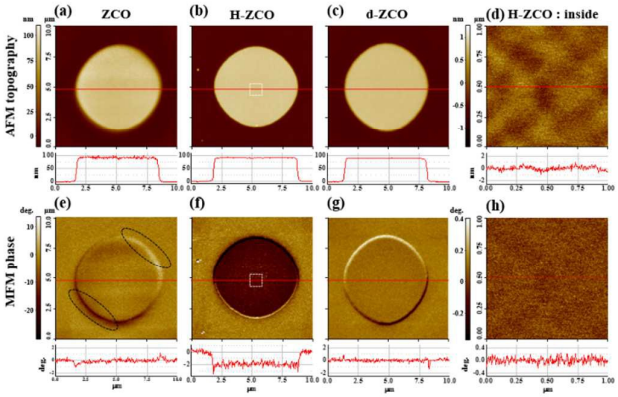

Fig. 4 (a)-(c) Atomic force microscopy (AFM) topography images and their line profile results, and (e)–(g) Magnetic force microscopy (MFM) phase images and their line profile results of ZCO, H-ZCO, and d-ZCO, respectively. The changes shown in the MFM image of the ZCO series reveal on/off switching of its magnetic domains by hydrogen mediation. The magnetic contrast near the circumference of the microdisk (marked by dotted black ellipses in (e)) do not originate from the change in magnetization, but instead, a topographic noise signal which appears to be dependent on the scan direction in MFM phase images. (d) and (h) Enlarged images of regions marked with dotted white boxes in (b) and (f), respectively.

supported the perpendicular magnetization configuration of H-ZCO microdisk as shown in Fig. 3(a) and (c). However, all of the H-ZCO microdisks exhibited perpendicular magnetization, regardless of the volume. The observed magnetic moment-up/ down phenomena of perpendicular magnetic domains make the encoding of binary spin information possible. At the present, the manipulation of the magnetic moments is only possible for the entire H-ZCO microdisk array; however, individual magnetic moment control of each micro-dot is expected to be introduced in the near future.

Figure 4 shows topography and magnetic-phase images of the ZCO series measured by atomic force microscopy (AFM) and magnetic force microscopy (MFM), respectively, at room-temperature. To observe magnetic domain structures, all samples were measured in the absence of an external magnetic field after saturation with a 0.55-T permanent magnet, along the out-of-plane magnetic easy-axis. Magnetic anisotropy of Co-doped ZnO system is still controversial [37-40]; however, our H-ZCO system has the easy-axis in the c-axis direction. The MFM tip was also magnetized along the axis of their apex in order to be sensitive to the out of plane component of the magnetic stray field of magnetic moments. In AFM image of ZCO (Fig. 4(a)), the diameter, height, and surface roughness of a ZCO microdisk were 7 μm, 80 nm, and 4.71 nm, respectively. After hydrogen injection at high temperature and pressure by hot isostatic pressing (HIP), the surface roughness of H-ZCO was decreased to 1.75 nm, while the changes in the diameter

View Article Online
DOI: 10.1039/C6RA05746B

and height were negligible (Fig. 4(b)). Even after hydrogen ejection, the overall structure of d-ZCO was not changed (Fig. 4(c)). However, significant changes were observed in MFM images indicated at each post-treatment step. Before hydrogen injection, ZCO had no magnetic phase contrast (Fig. 4(e)); the magnetic contrast observed in the region marked by dotted black ellipses was caused by a sudden topographic change and could be reversed depending on the MFM scan direction.[41] This unintended topographic noise signal was also observed for H-ZCO and d-ZCO (Figs. 3(d), 4(f) and (g)). In contrast to ZCO, ferromagnetic H-ZCO showed a distinct magnetic phase shifts in the disk area, as shown in Fig. 4(f). In the magnetic line profile of Fig. 4(f), the magnetic component along the out-of-plane axis was uniform through the entire magnetic domain, with a clear magnetic phase difference of ~2°. In d-ZCO which had been dehydrogenated, the perpendicular magnetic domain image clearly disappeared. These results are consistent with those of the magnetization–magnetic field strength (M–H) curves obtained (Fig 1(d)) well. For more detailed analysis, the precise magnetic domains of H-ZCO was investigated in a 1 μm x 1 μm area. Figures 4(d) and (h) are the enlarged AFM and MFM images of the regions marked by dotted white boxes in Figs. 4(b) and (f), respectively. Figure 4(d) had a surface roughness of 0.285 nm. Figure 4(h) shows a homogeneous magnetic phase distribution of 0.018° without any domain features. Moreover, in repetitive AFM and MFM measurements for several different regions, no significant difference was observed in the magnetic phase.

Conclusions

In conclusion, we produced well-defined magnetic H-ZCO microdisk array through the lift-off process. Hydrogen injection into ZCO samples was induced using a hydrogenation process and post-annealing treatments were used for hydrogen ejection from H-ZCO samples under ultrahigh vacuum conditions. MFM observation of H-ZCO microdisks provided clear evidence of out-of-plane magnetic moments. This phenomenon was reversible, which was demonstrated by the disappearance of magnetic domains following hydrogen ejection. The MFM images of the reversible out-of-plane magnetic moments were consistent with the results obtained from OOMMF simulations. The perpendicular magnetization was stable and independent of the domain size in the range of 2–10 μm. The perpendicularly polarized magnetization was reversed by applying an opposite external field, which remained after the removal of the field. This suggests the application of this material and fabrication technique to the development of novel transparent spintronic devices based on oxides, such as information storage and logic circuits.

Acknowledgements

This work was supported by a 2-Year Research Grant of Pusan National University.

Notes and references

1 A. Cho, *Science* 2002, **296**, 246.
2 J. Åkerman, *Science* 2005, **308**, 508
3 S. A. Wolf, D. D. Awschalom, R. A. Buhrman, J. M. Daughton, S. von Molnár, M. L. Roukes, A. Y. Chtchelkanova and D. M. Treger, *Science* 2001, **294**, 1488.
4 I. Žutić, J. Fabian and S. Das Sarma, *Rev. Mod. Phys.* 2004, **76**, 323.
5 D. D. Awschalom and M. E. Flatté, *Nat. Phys.* 2007, **3**, 153.
6 D. A. Allwood, G. Xiong, C. C. Faulkner, D. Atkinson, D. Petit and R. P. Cowburn, *Science*, 2005, **309**, 1688.
7 L. Thomas, M. Hayashi, X. jiang, R. Moriya, C. Rettner and S. S. P. Parkin, *Nature* 2006, **443**, 197.
8 S. S. P. Parkin, M. Hayashi and L. Thomas, *Science* 2008, **320**, 190.
9 E. R. Lewis, D. Petit, L. O'Brien, A. Fernandez-Pacheco, J. Sampaio, A-V. Jausovec, H. T. Zeng, D. E. Read and R. P. Cowburn, *Nat. Mater.* 2010, **9**, 980.
10 M. Donalto, C. Tollan, J. M. Porro, A. Berger and P. Vavassori, *Adv. Mater.* 2013, **25**, 623.
11 R. P. Cowburn, and M. E. Welland, Science, 2000, **287**,1466.
12 X. -P. Huang, Z. -L. Shi, M. Wang, M. Konoto, H. -S. Zhou, G. -B. Ma, D. Wu, R. Peng and N. -B. Ming, *Adv. Mater.* 2010, **22**, 2711.
13 I. M. Miron, T. Moore, H. Szambolics, L. D. Buda-Prejbeanu, S. Auffret, B. Rodmacq, S. Pizzini, J. Vogel, M. Bonfim, A. Schuhl and G. Gaudin, *Nat. Mater.* 2011, **10**, 419.
14 J. H. Franken, H. J. M. Swagten and B. Koopmans, *Nat. Nanotech.* 2012, **7**, 499.
15 T. Koyama, D. Chiba, K. Ueda, K. Kondou, H. Tanigawa, S. Fukami, T. Suzuki, N. Ohshima, N. Ishiwata, Y. Nakatani, K. Kobayashi and T. Ono, *Nat. Mater.* 2011, **10**, 194.
16 M. Yamanouchi, D. Chiba, F. Matsukura and H. Ohno, *Nature* 2004, **428**, 539.
17 M. Yamanouchi, J. Ieda, F. Matsukura, S. E. Barnes, S. Maekawa and H. Ohno, *Science* 2007, **317**, 1726.
18 C. Gould, K. Pappert, G. Schmidt and L. W. Molenkamp, *Adv. Mater.* 2007, **19**, 323.
19 L. Thevenard, A. Miard, L. Vila, G. Faini, A. Lemaître, N. Vernier, J. Ferré and S. Fusil, *Appl. Phys. Lett.* 2007, **91**, 142511.
20 Y. Matsumoto, M. Murakami, T. Shono, T. Hasegawa, T. Fukumura, M. Kawasaki, P. Ahmet, T. Chikyow, S. Koshihara and H. Koinuma, *Science* 2001, **291**, 854.
21 J. M. D. Coey, M. Venkatesan and C. B. Fitzgerald, *Nat. Mater.* 2005, **4**, 173.
22 K. R. Kittilstved, W. K. Liu and D. R. Gamelin, *Nat. Mater.* 2006, **5**, 291.
23 S. B. Ogale, *Adv. Mater.* 2010, **22**, 3125.
24 T. S. Herng, M. F. Wong, D. Qi, J. Yi, A. Kumar, A. Huang, F. C. Kartawidjaja, S. Smadici, P. Abbamonte, C. Sánchez-HanKe, S. Shannigrahi, J. M. Xue, J. Wang, Y. P. Feng, A. Rusydi, K. Zeng and J. Ding, *Adv. Mater.* 2011, **23,** 1635.
25 C. H. Park and D. J. Chadi, *Phys. Rev. Lett.* 2005, **94**, 127204.
26 H. -J. Lee, C. H. Park, S. -Y. Jeong, K. -J. Yee, C. R. Cho, M. -H. Jung and D. J. Chadi, *Appl. Phys. Lett.* 2006, **88**, 062504.
27 S. Lee, Y. C. Cho, S. -J. Kim, C. R. Cho, S. -Y. Jeong, S. J. Kim, J. P. Kim, Y. N. Choi and J. M. Sur, *Appl. Phys. Lett.* 2009, **94**, 212507.
28 Y. C. Cho, S. -J. Kim, S. Lee, S. J. Kim, C. R. Cho, H. -H. Nahm, C. H. Park, I. K. Jeong, S. Park, T. E. Hong, S. Kuroda and S. -Y. Jeong, *Appl. Phys. Lett.* 2009, **95**, 172514.

View Article Online
DOI: 10.1039/C6RA05746B

29 S. J. Kim, S. Lee, Y. C. Cho, Y. N. Choi, S. Park, I. K. Jeong, Y. Kuroiwa, C. Moriyoshi and S. -Y. Jeong, *Phys. Rev. B* 2010, **81**, 212408.
30 Y. C. Cho, S. Lee, H. H. Nahm, S. J. Kim, C. H. Park, S. Y. Lee, S. -K. Kim, C. R. Cho, H. Koinuma and S. -Y. Joeng, *Appl. Phys. Lett.* 2012, **100**, 112403.
31 J. M. Shin, H. S. Lee, S. Y. Cha, S. Lee, J. Y. Kim, N. Park, Y. C. Cho, S. J. Kim, S. -K. Kim, J. -S. Bae, S. Park, C. R. Cho, H. Koinuma and S. -Y. Jeong, *Appl. Phys. Lett.* 2012, **100**, 172409.
32 Xiaojuan Ye, Denglu Hou, Wei zong, Chaktong Au and Youwei Du, *Science in China Series G: Physics, Mechanics & Astronomy* 2009, **52**, 21.
33 Devaraj Soundararajan, *Journal of Magnetics* 2011 **16**, 216.
34 M. N. Lin, H. S. Hsu, J. Y. Lai, M. C. Guo, C. Y. Lin, G. Y. Li, F. Y. Chen, J. J. Huang, S. F. Chen, C. P. Liu and J. C. A. Huang, *Appl. Phys. Lett.* 2011, **98**, 212509.
35 S. Lee, W. -K. Kim, Y. C. Cho, B. -S. Kim, J. H. Park, C. -W. Lee, Y. Lee, S. Lee, S. Fackler, I. Takeuchi, C. R. Cho and S. -Y. Jeong, *Appl. Phys. Lett.* 2014, **104**, 052405.
36 S. Lee, J. H. Park, S. -Y. Jeong *Phys. Rev. Lett.* to be submitted.
37 M. Venkatesan, C. B. Fitzgerald, J. G. Lunney and J. M. D. Coey, *Phys. Rev. Lett.* 2004, **93**, 177206.
38 A. Dinia, G. Schmerber, C. Mény, V. Pierron-Bohnes and E. Beaurepaire, *J. Appl. Phys.* 2005, **97**, 123908.
39 P. Sati, R. Hayn, R. Kuzian, S. Régnier, S. Schäfer, A. Stepanov, C. Morhain, C. Deparis, M. Laügt, M. Goiran and Z. Golacki, *Phys. Rev. Lett.* 2006, **96**, 017203.
40 Z. Yang, M. Biasini, W. P. Beyermann, M. B. Katz, O. K. Ezekoye, X. Q. Pan, Y. Pu, J. Shi, Z. Zuo and J. L. Liu, *J. Appl. Phys.* 2008, **104**, 113712.
41 A. Wadas and H. -J. Güntherodt, *J. Appl. Phys.* 1990, **68**, 4767.